TASK QUARTERLY 7 No 4 (2003), 525–538

LOADS ON WALLS AND INSERTS IN MASS-FLOW SILOS

SONGXIONG DING, MICHAŁ WÓJCIK, MLADEN JECMENICA AND SUNIL R. DE SILVA

Department of Process Technology, Tel-Tek,
Telemark Univerity College,
N-3914 Porsgrunn, Norway
{*Songxiong.Ding, Michal.Wojcik, Mladen.Jecmenica, Sunil.DeSilva*}*@hit.no*

(Received 8 September 2003)

Abstract: A finite element analysis has been carried out to investigate flow patterns and loads on silos either with a ralatively steep hopper, or with a shallow hopper but in the presence of an insert. A Lagrangian-Eulerian approach was first adopted to simulate the material flow pattern. With the precondition that mass flow was obtained, it was then attempted to predict the loads exerted by granular materials on the walls of such silos. The load on the insert was also simulated. Techniques such as the adoption of adaptive meshes and filleting along sharp corners were applied in the analysis to overcome the difficulties usually encountered with large deformations in the FEM and the mathematic singularity presented by the abruptness of geometry. Filleting proved to be necessary to bring down the pressure peak at the transition level. The insert took over a significant part of the loads. Comparison with the classic theories have confirmed that the loads predicted on the wall agree quite well with the theoretical results in the silo's cylinder section, but that differences exist in the hopper section; the difference is greater when the hopper is shallower. It has also shown the limitations of predicting flow patterns of granular materials with the traditional elastic-plastic model; a more advanced model is needed.

Keywords: silo flow/loads, insert, Lagrangian-Eulerian, adaptive, fillet

1. Introduction

The flow patterns and the loads exerted on the walls during silo discharge have been the topics of extensive theoretical and experimental research worldwide. It has been recognised that the loads cannot be predicted without the knowledge of the flow pattern. However, the flow pattern itself is still difficult to predict.

Two kinds of flow patterns are recognised, namely mass flow and funnel flow. Mass flow is a flow mode in which every particle in a silo is in motion once discharge starts. Funnel flow is a flow mode where stationary zones exist in certain parts of a silo, most likely above the hopper walls. Each of these flow modes has its advantages. Based on material properties measured, for example, with the Jenike Cell, criteria have been established to predict whether a silo functions in mass flow or funnel flow, as long as its

geometry is relatively simple [1–3], even though the prediction of size and whereabouts of the boundaries of stationary zones in funnel flow is still unsatisfactory [1, 4, 5].

In the determination of wall loads for silo structural design, considerable uncertainty still persists because of the complexity of the pressure pattern, mostly due to funnel flow. Up to now, there has been little international agreement on a unified standard, even though many such attempts are currently being made [6, 7]. One still has to rely on a formula developed by Janssen in 1895 [8] and its modifications [9–12]. When mass flow is obtained, the Janssen formula can be used to predict the loads of granular materials on the walls of a silo with a simple geometry. But when more complex situations are involved, for example the presence of an insert, a device commonly used to convert a funnel flow silo into a mass flow silo, the Janssen formula appears to be inadequate.

The last two decades have seen many attempts at developing computational models to represent the behaviour of granular materials in silos. One of the most commonly used methods has been the finite element method. In FEM, a granular material is represented as a continuum with an appropriate constitutive law; the analysis may be static or dynamic, and is carried out according to the Eulerian [13, 14], the Lagrangian [15] or the Eulerian-Lagrangian approach [16]. General progress has recently been made in predicting macroscopic phenomena such as the flow behaviour of granular materials and the reaction of a wall under pressure exerted by granular materials. However, it has also become evident that this method has its limitations [17]; for instance, the continuum approach does not permit any behaviour occuring at the scale of individual particles. Another, even more common difficulty is to represent the mesh being massively distorted by large deformations and an abrupt change of direction at the transition from the cylinder section to the hopper section of a silo [18, 19].

In this paper, attempt has been made to tackle the difficulties due to the large deformations and the direction abruptness of a silo involved in discharging. The flow modes a silo may give have been addressed. Predictions of loads exerted on the wall have also been made after mass flow was obtained. In order to achieve this, two axi-symmetrical silos were assumed. Both had the same cylinder section, one with a relatively steep hopper, the other with a shallow hopper. A double-cone insert was introduced into the silo with the shallower hopper. In the end, the predicted results were compared with those from the most commonly quoted references.

2. Silo geometries and contents

The silo with a steeper hopper had a cylindrical section, which was 6 m in height and 2.5 m in diameter. The hopper was 3.94 m high, with a 15° angle and an outlet 0.41 m in diameter (Figure 1a). The wall was 6 mm thick, for both the hopper and the cylinder. The silo with a shallow hopper had the same cylinder, but the hopper was 1.5 m high with a 35° angle (Figure 1b). Its wall thickness was also 6 mm for both the hopper and the cylinder. In the shallow silo, a double-cone insert was installed as shown in Figure 1c, aligned with the silo's axis. The dimensions of the insert are shown in the same figure. The material was filled to a height of 2 m below the silo top, with an additional 25° conical heap on top.

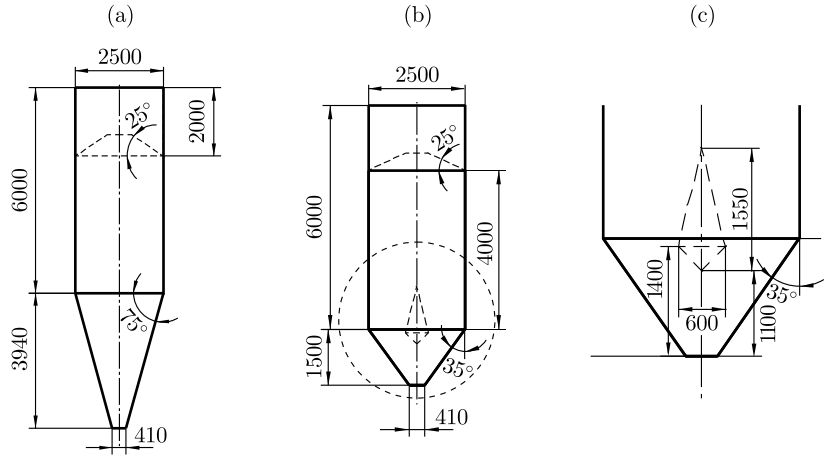

Figure 1. Configurations of the simulation conditions: (a) silo with steep hopper, (b) silo with shallow hopper, (c) a double-cone insert

3. Finite element modelling

The geometries as shown in Figure 1 were discretized, and finite element meshes were adopted as follows:

1. rigid elements were used to represent the insert;
2. axi-symmetrical shell elements represented the wall;
3. the granular material was treated as solid elements, and continuum axi-symmetrical elements were designed for the material region.

These constitute the element domain. Upon the element domain, the silo wall was fixed at its transition level between the hopper and the cylinder section, and constrained horizontally at its top. The loading of the granular material was due to its gravity, but the silo wall was assumed to be weightless.

In the model, the silo wall was assumed to be made of steel and was modelled as an elastic material, with Young's modulus, E_w, and Poisson's ratio, ν_w, set at $2 \cdot 10^{11}$ Pa and 0.25, respectively. The insert was represented as a rigid surface. Granular materials display quite complicated behaviour. The identification of a material model remains open. It is still a challenge to generalise a constitutive law. However, this is not the main purpose of the present study, where the widely accepted elastic-plastic model was utilised.

The interaction between the material and the wall depends on the material of the wall and the properties of the granular material. Modelling such a mechanical interaction can be quite complex. In the paper, a suggested Coulomb interface, which is necessary for mass flow, has been adopted to model the friction between the granular material and the wall surface [20, 21] and between the granular material and the insert surface, when the insert is used. A constant friction coefficient has been defined and implemented in the model.

4. Numerical analysis

4.1. Convergences and determination of parameters

Convergence has been a precondition for ABAQUS analysis. It is a complex issue and has been well discussed in the ABAQUS manual. In the present study, convergence is mostly relevant to mesh design, contact definition and the significant deformation undergone during discharge.

Both coarse and fine meshes were designed and tried. In order to obtain a better mesh domain, partition was used in the material region in order to design finer meshes in key areas. The abrupt geometry change at the transition from the cylinder to the hopper presents a serious numerical problem and leads to a mathematical singularity [22, 23]. A smoothing technique was therefore conducted to avoid any sharp corners [19]. The silo transition was curved into a smoothed curvature with radii of 0.5m and 1m, and a 0.1m radius was designed at the corner of the insert. After such modifications of geometry, the mesh was redesigned as shown in Figure 2, as an example.

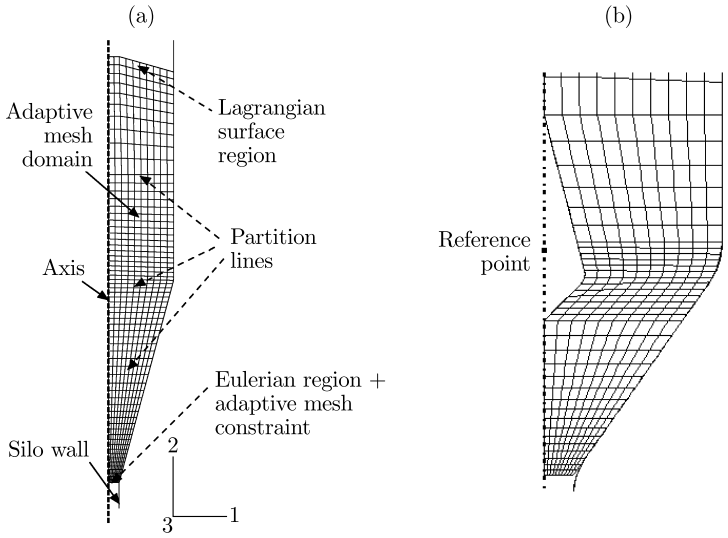

Figure 2. The meshes designed, with modifications: (a) Lagrangian-Eulerian approach, (b) filleting applied to areas with abrupt geometry

Based on the modified meshes, the interaction between wall and material was defined by the friction occurring along the contacting surfaces of elements. As has been mentioned, the implementation of contact was complicated. Many warnings were issued when the default kinematic method frictional constraint was imposed, and the running of the programme was interrupted right at the beginning. This was overcome after changing the kinematic method frictional constraint into the penalty method restraint [20].

The deformation the material would undergo depends on the setting of parameters for the material. For instance, the gravity loading was defined through density. It makes the material deform, and therefore has an influence on the numerical con-

vergence in a combination of the material's Young modulus, E_w, Poisson's ratio and its yield stress.

The setting of material parameters was related to the elastic-plastic model. In this research, the measurable parameters were based on the Mohr-Coulomb model for a granular material. They were the material internal friction angle, φ, and its friction angle with the wall, ϕ, set at 30° and 18°, respectively. Young's modulus, E_w was charted from references [24, 25] for the granular material, and the Poisson ratio, ν_p, was given by [26] as 0.33.

Convergence tests were carried out with a density of $\rho = 1\,000\,\mathrm{kg/m^3}$ for the particulate material, and convergence was achieved when Young's modulus, E_w, was higher than $7.0 \cdot 10^5\,\mathrm{Pa}$ in a preliminary simulation, where the material was assumed with a Mohr-Coulomb limitation. With the kinematic hardening limitation, Young's modulus could be as low as $4.3 \cdot 10^5\,\mathrm{Pa}$. The other parameters had little effect on convergence.

In the simulations reported here, the results were based on those from the denser meshes. The parameters used were: material density $\rho = 1\,000\,\mathrm{kg/m^3}$, Young's modulus $E_w = 10^6\,\mathrm{Pa}$; the Poisson ratio $\nu_p = 0.3$; the material's internal friction angle $\varphi = 30^\circ$, while the wall's friction angle, ϕ, was 18° for the M-C model. The parameters were consistent with references [24, 25].

4.2. Determination of flow pattern

4.2.1. Lagrangian-Eulerian approach

In the discharging process, the amount of material left inside the silo decreases; as a result, the boundaries of the material body are changing. Such a process is a complicated problem concerning the FEM formulation involved. To properly cope with it, an arbitrary Lagrangian-Eulerian formulation approach is required. At the outlet, the material is discharged either freely or in a controlled way, for which a fixed boundary could be prescribed: an Eulerian approach is favourable. In the other regions, the boundaries are moving with the material, and a Lagrangian approach is needed.

To apply these approaches, an adaptive mesh was defined for the material domain. Upon this domain, a zero movement of adaptive mesh constraint and an Eulerian surface region were applied to the boundary of the outlet. By doing so, the meshes at the outlet were fixed, but the material can still flow through across these meshes. A Lagrangian-type region was applied to the other boundaries in order to ensure that the edges of the mesh follow the movement of the material. They are illustrated in Figure 2. The application of the adaptive meshes has been proven to be an effective technique to deal with the difficulty of mesh distortion caused by the large deformation in the process of discharging.

4.2.2. Discharging flow pattern

A Lagrangian-Eulerian approach was used to simulate the material's movement during discharge. Having set up the boundaries as above, the challenge was to prescribe an initial condition to simulate the stresses in the material's storage state. These stresses were essentially developed during filling. Attempts to import the stress distributions from the simulation results for filling were unsuccessful

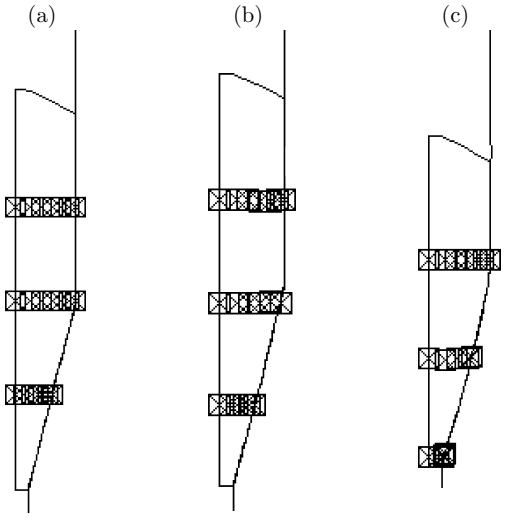

Figure 3. Tracer movements at various stages of discharge in the silo with the steep hopper: (a) tracers at the beginning, (b) tracers at middle stage, (c) tracers at final stage

because a bug called "a floating-point invalid operation" was encountered during the process of importation. (Reportedly, this bug has been solved in the latest version of ABAQUS 6.4 [27]). Alternatively, the initial condition adopted in the current analysis was the stresses at the top surface and along the outlet obtained from the theoretical formula for the silo's active state of stress, *i.e.* 0.0Pa at the top surface with different values along the outlet for calculated the steep and the shallow silos (see Appendix).

Since the adaptation of the adaptive meshes, the movement and deformation of the meshes by definition no longer represented the material's movement. Tracers were seeded along the partition lines in order to monitor the material movement. Since the tracers would require very long computation, only limited numbers of tracers were used.

A free discharge process was simulated and several parallel tests were carried out. The material model first implemented was the elastic-plastic one with M-C limitation. Satisfactory results were achieved for the steep silo, as shown in Figure 3, for the movement of the tracers. The tracers in the hopper moved faster than those in the cylinder; the tracers closer to the centre moved faster than those closer to the hopper wall, while the tracers moved with the same speed when they were in the cylinder. Various wall friction values were used, but they produced no difference in flow patterns. The tracer movements indicate that mass flow was achieved. However, the tracer movements in the shallower hopper (with or without insert) were not very realistic, with some of the tracers even moving upwards.

Further simulations were then carried out after implementing the elastic-plastic material model with kinematic hardening. In Figure 4, some of the results are shown for tracers' movements in both silos, and the shallow silo with the insert. Results similar to those described above were achieved for the silo with the steep hopper. In the silo with the shallow hopper, the tracers adjacent to the wall did not move, while the others did move, and the tracers close to the centre were faster than those close to the wall, but the tracers on the higher level moved faster than those on the

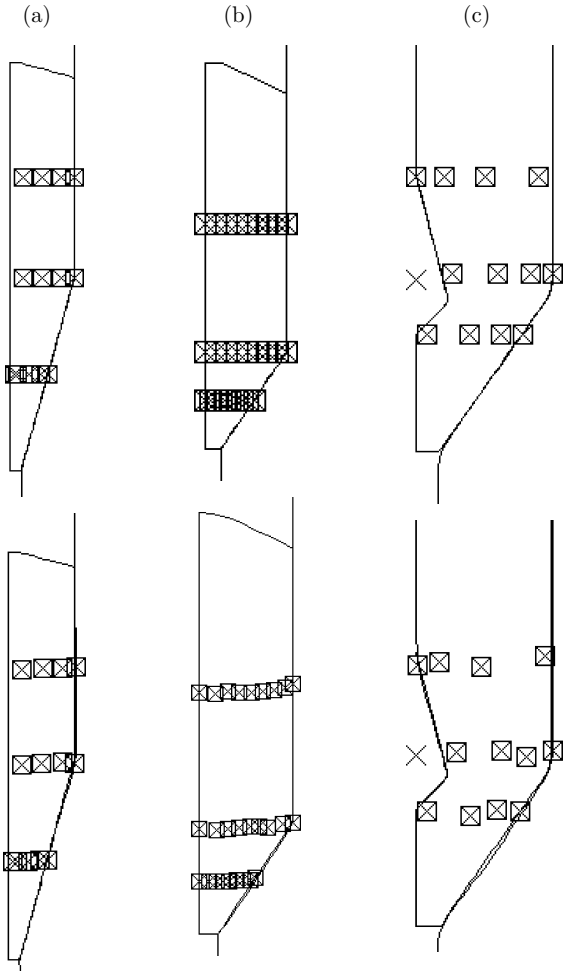

Figure 4. Tracer positions in the beginning of discharge (upper) and at various stages of the simulation (lower) for the three silo geometries (wall friction 0.6 for all cases): (a) in the silo with the steep hopper, the tracers close to centre moved faster than those close to the hopper wall, but with the same velocity when they were in the cylinder section; (b) in the silo with the shallow hopper, without insert, the tracers adjacent to the wall did not move. The tracers close to centre moved faster than those close to the wall; (c) in the silo with the shallow hopper and the insert, all tracers moved; the tracers in the middle moved faster than the others

lower level. This was attributed to the initial stresses and various initial conditions were tried out, but without decisive achievements so far. With the installation of the double cone into the shallow hopper, all tracers started to move. The tracers in the middle moved faster than those close to the wall and the insert. But, again, the tracers on the higher level moved faster than those on the lower level. Various initial conditions were also tested without improvement. So far, one can see that mass flow was achieved for the silo with the steep hopper; for the silo with a shallow hopper in the presence of an insert, further attempts were made with another code, called SILO [14].

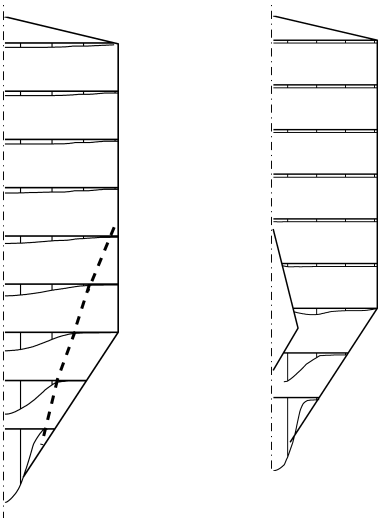

Figure 5. Change of flow pattern in the silo with the shallow hopper in the presence of the insert

4.2.3. Application of the SILO code

The SILO code, based on a continuum model, was developed at Luleå University of Technology, Sweden. It was modified and implemented at the University of Telemark, Norway. This model adopted an Eulerian approach, suitable for situations where steady-state flow was reached in silos. This steady-state was used to investigate the granular material flow in a silo, and the effects of inserts on such flow. Numerical simulations were carried out to predict granular flow patterns for the condition of the silo with the shallow hopper, in the presence or absence of the double-cone insert. The results are show in Figure 5.

On the left of Figure 5, one can see that a substantial stagnant zone (about 1/3 height of the cylinder section and 1/3 in radius from the transition edge as divided along the dashed line) developed around the transition region when there was no insert. Compared with the results on the left, it is easy to see that the installation of the double-cone changes the material's flow pattern. In the cylinder section, the material moved quite evenly. Below the transition level, however, the material close to the wall moved much slower than that closer to the centre. No stagnant zones existed anymore, even though the flow was still not a mass flow in the strict sense.

4.3. Prediction of loads

With the precondition that a mass flow pattern was achieved, simulations were then carried out to predict the loads exerted by the granular material on the wall and the surface of the insert. In a mass flow silo, all particles started to move at the commencement of discharge. At that moment, there is a significant pressure shift. During this shift, the highest pressure will most likely develop when the flow channel is fully activated. An analysis was thus carried out of the change occurring during this period. The material model was the elastic-plastic model with M-C limitation.

Taking advantage of the meshes designed as shown in Figure 2, an ABAQUS analysis was carried out by applying gravity loading to the region of the material

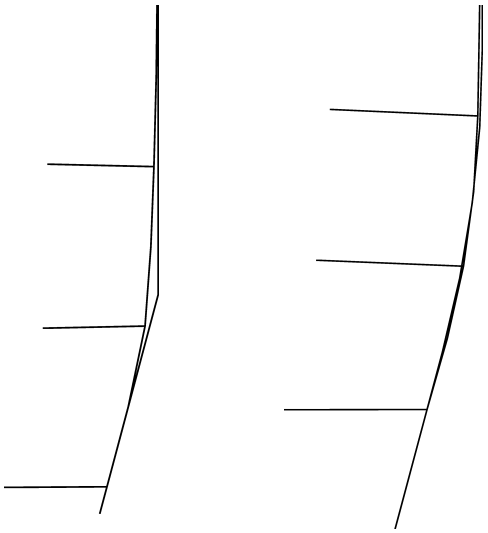

Figure 6. When the material deforms, it separates from the wall at the transition; this leads to line contact below with a very high pressure peak

when the outlet was just opened. The material deformed, and particularly severe deformation was observed at the transition. The deformation led to a separation of the material from the wall. Figure 6 shows examples of such separation, which occurred at the transition of the steep silo with no fillet (left) and with a 0.5 m fillet (right).

Below the separation, there were contact pressure peaks. These peaks could be very high ($8 \cdot 10^5$ Pa for the shallower hopper and $5 \cdot 10^5$ Pa for the steep hopper) due to point (line) contact between the material and the wall when there was no fillet at the transition. These line contacts were modified into surface contacts by the application of filleting of the corners. After such modifications, the peaks dropped close to and even lower than the theoretically predicted peaks, as shown in Figure 7.

Figure 7 shows the contact pressures along the walls for the silo with the steep hopper (a) and for the silo with the shallow hopper in the presence of the insert (b). Both were plotted along with the results predicted by the classic theories referred to in the Appendix. The loads on the surface of the insert are shown in Figure 8.

It is apparent from Figure 7 that the results from ABAQUS simulations for the two radii, 0.5 m and 1 m, of filleting at the transition are similar; and that the insert had a significant load. Overall, as has been seen, the results predicted in both cases by ABAQUS agreed quite well with the theoretical results in the silo's cylinder section, but differences existed in the hopper section, especially for the shallower hopper with the insert. Since the theoretical formulae were developed only for hoppers without an insert, the comparisons for this type of hopper are, strictly speaking, not valid. Before reaching the peaks, the pressure calculated with ABAQUS dropped to zero. It was due to the separation shown in Figure 6. When there was no contact, the pressure would be zero.

It is also interesting to observe the effect the insert had on the wall pressures. Referring to the results shown in Figure 8, one finds that the insert took a significant part of the load. A comparison of the maximum contact pressure in the steep hopper

(a)

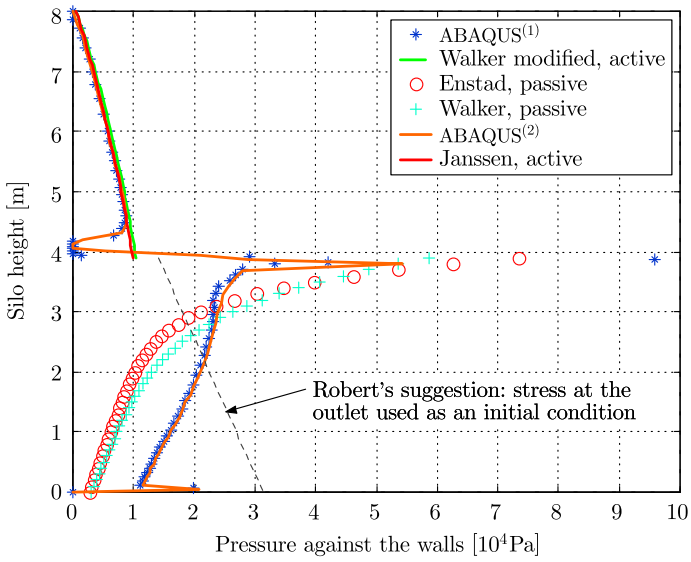

(b)

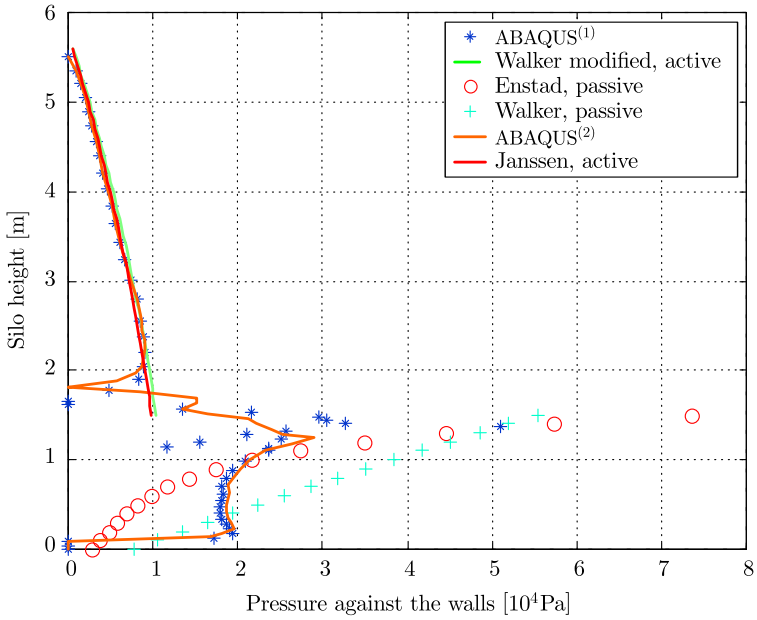

Figure 7. Predictions of pressure along the wall: (a) comparisons between ABAQUS™ predictions and theoretical results in the steep hopper silo; (b) comparisons between ABAQUS™ predictions and theoretical results in the shallow hopper silo with the double-cone insert. The effect of the insert is ignored in the calculations according to the Walker and Enstad theories; (1) – fillet radius 0.5m, (2) – fillet radius 1.0m at the transition of the silo

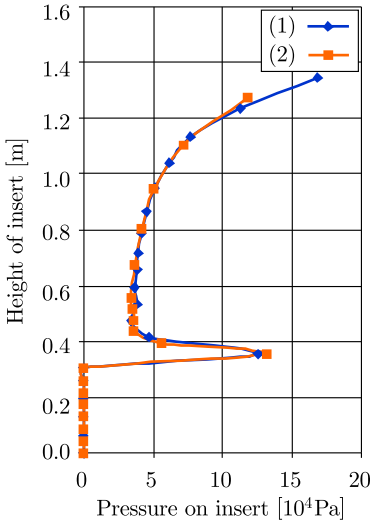

Figure 8. Predictions of pressure on the insert:
(1) – inclination of hopper wall = 35°, fillet radius = 1.0m,
(2) – inclination of hopper wall = 35°, fillet radius = 0.5m

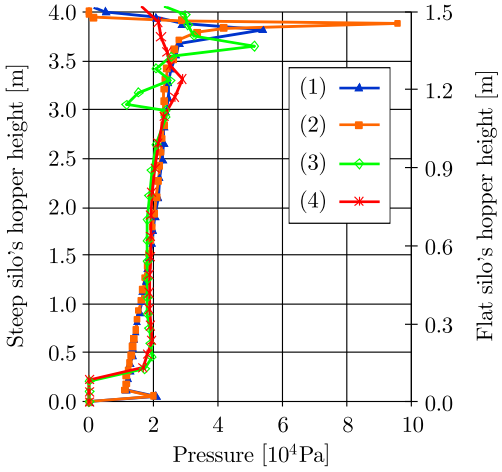

Figure 9. The insert significantly decreases the pressure peak at the transition:
(1) – inclination of the hopper wall = 15°, fillet radius = 1.0m,
(2) – inclination of the hopper wall = 15°, fillet radius = 0.5m,
(3) – inclination of the hopper wall = 35°, fillet radius = 0.5m,
(4) – inclination of the hopper wall = 35°, fillet radius = 1.0m

with those in the shallow hopper (Figure 9) shows that the insert greatly decreased the pressure peak at the transition, even though there were no significant changes in other regions. The insert had some effect on the peak contact pressure. However, this decrease became less obvious when the fillet radius became larger.

5. Conclusions

The finite element analysis with ABAQUS was used to predict the flow and loads in silos in the present study. The study showed that the application of adaptive

meshes was effective in dealing with a process with a large deformation. By defining an adaptive mesh for the granular material and suitable constraining boundaries and surfaces for this mesh region, a Lagrangian-Eulerian approach was adopted to simulate the material discharging process with a degree of success. The factors crucial for obtaining proper predictions were a material model and proper determination of the relevant parameters. The current well-known elastic-plastic model has its limitations; more advanced models are required.

In the context of mass flow being achieved in silos with either a steep or a shallow hopper in the presence of a double insert, attempts have been made to predict the contact pressure exerted by the material on the insert and the wall. It has been shown that:

1. the insert took over a significant part of the load, and
2. the predicted pressures along the walls were in good agreement with the results obtained from theoretical formulae in the silos' cylinder section, but agreement was poor in the hopper section.

This difference in the hopper section was even more significant as the hopper became shallower. Such differences support the argument that the theoretical formulae are no longer suitable when the hopper becomes too shallow and the geometry becomes complex due to the presence of an insert. However, good agreement should not be expected in such circumstances. Strictly speaking, the theoretical formulae were only derived for hoppers without inserts, and the calculations with these formulae for the shallower hopper with the insert were therefore not entirely valid. However, this argument is not meant to prove that the simulation results are correct either. It is a matter for further experimental verification.

It has also been shown important to apply filleting to regions with sharp corners in the geometry to avoid mathematic singularities and thus improve the conditions to achieve convergence in FEM analysis. The fillet modified line contact into surface contacts and thus reduced the contact pressure peak which would otherwise develop. However, it remains to be seen whether this is peculiar for simulations or whether it also occurs in practice.

Appendix: The most commonly quoted classic theories

There is a number of theories to predict silo wall pressures induced by the stored material. A brief review of the most commonly quoted ones is given below; they were used in the text for comparison.

The cylinder section: the Janssen and Walker formula

Janssen's original analysis was carried out on a cylindrical bunker containing a cohensionless granular material. He derived the pressure against the wall as expressed with:

$$\sigma_{rr} = \frac{\gamma D}{4\mu_w}\left[1-\exp\left(-\frac{4\mu_w K z}{D}\right)\right]+\frac{\gamma D K}{6}\tan\eta\exp\left(-\frac{4\mu_w K z}{D}\right), \qquad (1)$$

where γ is the granular material's specific weight, [N/m^3], D – the silo diameter, [m], $\mu_w = \tan\phi$ – the material's friction against the wall, ϕ – the material's friction angle with the walls, and K is the Janssen constant, defined as follows:

$$K = \frac{\sigma_{rr}}{\sigma_{zz}}. \tag{2}$$

σ_{zz} is the average vertical stress along a horizontal plane z of the cylinder, z is the material's height from the top, and η is the angle of repose.

Walker improved the Janssen equation by reconsidering in greater detail the actual stress distribution in the wall region and the cross-section, as well as by modifying the K constant into K_{wa}, as in Equation (3) below:

$$K_{wa} = \frac{1-\sin\varphi\cos(\omega-\phi)}{1+\sin\varphi\cos(\omega-\phi)}, \tag{3}$$

where

$$\omega = \arcsin\left(\frac{\sin\phi}{\sin\varphi}\right), \tag{4}$$

φ – the material's internal friction angle.

The hopper section: the Walker and Enstad formulae

Janssen's analysis was extended to the hopper by Walker and Enstad [9, 11]. In Walker's analysis, it was assumed that the vertical stress is constant across any horizontal cross-section. Using the slice element method, he offered the following solution of the pressure acting on the wall:

$$\sigma_w = (\sigma_{hh})_w \frac{1+\sin\varphi\cos(\omega+\phi)}{1-\sin\varphi\cos(\omega+\phi+2\alpha)}, \tag{5}$$

where

$$(\sigma_{hh})_w = \Omega\left\{\frac{\sigma_{rr}}{K}\left(\frac{h}{h_0}\right)^m + \frac{\gamma h}{m-1}\left[1-\left(\frac{h}{h_0}\right)^{m-1}\right]\right\}. \tag{6}$$

Ω is a distribution factor as the ratio of the axial stress at the wall and the mean axial stress. σ_{rr} is the result from Equation (1); h – the height of material measured vertically from the apex of the hopper, [m]; h_0 – the maximum of h in the hopper, [m];

$$m = \frac{2\sin\varphi\sin(\omega+\phi-2\alpha)}{\tan\alpha[1-\sin\varphi\cos(\omega+\phi+2\alpha)]}, \tag{7}$$

where α is the hopper's half angle.

Enstad assumed that the minor principal stress was constant across a spherical surface spanning the hopper, and by effort derived another approximation of the pressures in the hopper. Expressed in terms of the mean stress, his solution of the pressure induced by the material along the wall during flow was given as:

$$\sigma_w = p(1+\sin\varphi\cos 2\beta) \tag{8}$$

and

$$p = \frac{\gamma Y r}{X-1} + \left(\frac{\sigma_{rr}}{K(1-\sin\varphi)} - \frac{\gamma Y r_0}{X-1}\right)\left(\frac{r}{r_0}\right)^X, \tag{9}$$

where

$$X = \frac{2\sin\varphi}{1-\sin\varphi}\left[1+\frac{\sin(2\beta+\alpha)}{\sin\alpha}\right], \tag{10}$$

$$Y = \frac{\sin\beta \sin^2(\alpha+\beta) + 2[1-\cos(\alpha+\beta)]\sin\alpha}{(1-\sin\varphi)\sin^3(\alpha+\beta)}, \tag{11}$$

$$\beta = 0.5(\omega+\phi), \tag{12}$$

and r is the height of material measured radically from the apex of the hopper along the hopper wall, [m], while r_0 is the maximum of r in the hopper, [m].

References

[1] Jenike A W 1987 *Powder Technology* **50** (3) 229
[2] Drescher A 1998 *Phil. Trans. Royal Society of London: Series A-Math.* **356** (1747) 2649
[3] Drescher A 1992 *Powder Technology* **73** (3) 251
[4] Michalowski R L 1987 *Chem. Engng. Sci.* **42** (11) 2587
[5] Nedderman R M 1995 *Chem. Engng. Sci.* **50** (6) 959
[6] Roberts A W 1989 *Loads on Bulk Solids Containers*, Draft Australian Standard for Comment
[7] Rotter J M 1998 *Thin-Walled Structures* **31** (1-3) 3
[8] Janssen H J 1895 *Zeitschrift des Verein Deutscher Ingenieure* **39** (35) 1045
[9] Walker D M 1966 *Chem. Engng. Sci.* **21** 975
[10] Walters J K 1973 *Chem. Engng. Sci.* **28** 13
[11] Enstad G G 1981 *A Novel Theory on the Arching and Doming in Mass Flow Hoppers*, PhD Thesis, Norwegian Institute of Technology, Bergen
[12] Drescher A, Waters A J and Rhoades C A 1995 *Powder Technology* **84** (2) 165; *ibid.* 176
[13] Haussler U and Eibl J 1984 *J. Engng. Mech.* **110** (6) 957
[14] Karlsson T 1996 *Finite Element Simulation of Flow in Granular Materials*, Licentiate Thesis, Luleå University of Technology
[15] Martÿnez M A, Alfaro I and Doblare M 2002 *Engng. Structures* **24** 1561
[16] Nedderman R M and Tuzun U 1987 *Powder Technology* **22** 243
[17] Rotter J M, Holst J M F G, Ooi J Y and Sanad A M 1998 *Phil. Trans. Royal Society of London: Series A-Math.* **356** (1747) 2685
[18] Ooi J Y and Rotter J M 1990 *Computers & Structures* **37** (4) 361
[19] Ragneau E, Ooi J Y and Rotter J M 1998 *SILOS* (Brown C J and Nelsen J, Eds), E & FN SPON, pp. 495–508
[20] HIBBITT, KARLSSON & SORENSEN INC 2001 *ABASQUS Manual*
[21] Ooms M and Roberts A W 1985 *Bulk Solids Handling* **5** (6) 1271
[22] Ottosen N S and Petersen H 1992 *Introduction to the Finite Element Method*, Prentice Hall
[23] Zienkiewicz O C and Taylor R L 2000 *The Finite Element Method*, Butterworth-Heinemann
[24] Standards Association of Australia (SAA) 1990 *Loads of Bulk Solid Containers*, AS #774-, Sydney
[25] Hjelmstad K D and Taciroglu E 2000 *J. Engng. Mech., ASCE* **126** (8) 821
[26] Qu Q, Negi S C and Jofriet J C 2001 *Powder Handling Processing* **13** (1) 27
[27] Lind H 2003 *E-mail Exchanges and Discussions*, ABAQUS consultations in Scandinavia